

THE AMORPHIZATION OF CERAMICS BY ION BEAMS

DE85 000936

C. J. McHargue, G. C. Farlow, C. W. White, J. M. Williams, B. R. Appleton,
and H. Naramoto

Oak Ridge National Laboratory, Oak Ridge, Tennessee USA 37831

SUMMARY

The influence of the implantation parameters fluence, substrate temperature, and chemical species on the formation of amorphous phases in Al_2O_3 and α -SiC was studied. At 300 K, fluences in excess of 10^{17} ions \cdot cm $^{-2}$ were generally required to amorphize Al_2O_3 ; however, implantation of zirconium formed the amorphous phase at a fluence of 4×10^{16} Zr \cdot cm $^{-2}$. At 77 K, the threshold fluence was lowered to about 2×10^{15} Cr \cdot cm $^{-2}$. Single crystals of α -SiC were amorphized at 300 K by a fluence of 2×10^{14} Cr \cdot cm $^{-2}$ or 1×10^{15} N \cdot cm $^{-2}$. Implantation at 1023 K did not produce the amorphous phase in SiC. The micro-indentation hardness of the amorphous material was about 60% of that of the crystalline counterpart.

INTRODUCTION

The use of ion implantation to modify the near surface properties of ceramics such as Al_2O_3 and SiC has received increased attention in recent years [1-6]. Whereas the concentrations of dopants implanted in semiconductors are generally very low and complex radiation damage to the host lattice does not occur, the concentrations required for property alteration in metals and ceramics are in the 1 to 20 at. % range; hence, damage levels are high.

Implantation damage (irradiation damage) in ceramics is much more complex and less studied than in metals and semiconductors. In the displacement cascade, one must deal with at least two sublattices that may

NOTICE

PORTIONS OF THIS REPORT ARE ILLEGIBLE

It has been reproduced from the best available copy to permit the broadest possible availability.

By acceptance of this article, the publisher or recipient acknowledges the U.S. Government's right to retain a nonexclusive, royalty-free license in and to any copyright covering the article.

DISTRIBUTION OF THIS DOCUMENT IS UNLIMITED

MASTER

EHB

DISCLAIMER

This report was prepared as an account of work sponsored by an agency of the United States Government. Neither the United States Government nor any agency thereof, nor any of their employees, makes any warranty, express or implied, or assumes any legal liability or responsibility for the accuracy, completeness, or usefulness of any information, apparatus, product, or process disclosed, or represents that its use would not infringe privately owned rights. Reference herein to any specific commercial product, process, or service by trade name, trademark, manufacturer, or otherwise does not necessarily constitute or imply its endorsement, recommendation, or favoring by the United States Government or any agency thereof. The views and opinions of authors expressed herein do not necessarily state or reflect those of the United States Government or any agency thereof.

have different displacement energies. The types of defects that can be produced are strongly influenced by the requirements of local electrical charge neutrality, the local stoichiometry, and the nature of the chemical bonding of the particular lattice. In addition, ionizing effects may be significant in producing lattice defects, whereas in metals such effects are unimportant.

Naguib and Kelly [7] include Al_2O_3 in their list of materials that become amorphous during ion bombardment. This conclusion was based on results from gas-release studies [8], Rutherford backscattering (RBS) [9], and reflection electron diffraction patterns [10]. A transmission electron microscopy (TEM) study by Rehtin, however, indicated the structure of Al_2O_3 implanted with helium, oxygen, neon, or carbon to remain crystalline with a defect structure largely characteristic of that produced by electron or neutron irradiation [11]. Our previous work [1-4] as well as that of Burnett and Page [5] and Hioki et al. [6] have shown that high fluences are required to produce a near-surface amorphous phase in Al_2O_3 for substrate temperatures near 300 K.

A number of studies on $\alpha\text{-SiC}$ [see reference 12 for a review] have reported that the damage as measured by RBS-channeling saturates at a value corresponding to that of a random sample indicating an amorphous condition. However, Raman spectroscopy indicated some characteristic crystalline bonding might remain [13,14].

In order to clarify these issues, we are studying the effect of implantation parameters on the structure of Al_2O_3 and $\alpha\text{-SiC}$.

EXPERIMENTAL PROCEDURE

The Al_2O_3 substrates used in this work were single crystals with the (0001) orientation. These crystals were implanted off axis in a high

vacuum environment using current densities less than $2 \mu\text{A}/\text{cm}^2$ to minimize beam heating during implantation. The specimen holder could be cooled or heated to cover the temperature range of 77 to 700 K. Implanted impurity species included chromium and zirconium at energies chosen such that the peak in the as-implanted concentration profile was at a depth of about 800 Å. To simulate the effect of self-ion damage in the absence of any impurity, crystals were implanted with aluminum and oxygen ions in the stoichiometric ratio of 2 to 3. The energies of the aluminum and oxygen ions were chosen such that the peaks in the implanted profiles also occurred at the same depth ($\sim 800 \text{ Å}$).

Single crystals of $\alpha\text{-SiC}$ also in the (0001) orientation, were obtained by the Acheson furnace process at the Carborundum Company. They were implanted with nitrogen (62 keV) or chromium (280 keV) at room temperature and 1023 K.

The effects of implantation on the structural properties were evaluated using 2.0 MeV Rutherford backscattering and ion channeling measurements. Selected crystals were also examined by cross sectional TEM measurements. Near surface mechanical properties were evaluated using the Knoop micro-indentation hardness technique and single pass scratch tests. These results were correlated with the structural changes measured by RBS and TEM.

RESULTS AND DISCUSSION

The implantation parameters that were varied for the Al_2O_3 samples were temperature, fluence, and species of implant (mass and chemical effects). Figure 1 summarizes the RBS data for the chromium implants at 77 and 300 K. The data are presented as lattice damage, χ (aligned

yield/random yield in the aluminum-sublattice at the depth of the peak chromium concentration) versus fluence. At 77 K, the damage increased at an approximately linear rate up to a fluence of 10^{15} ions·cm⁻², then at a greater rate in the range of 1 to 2×10^{15} ions·cm⁻², indicating that the transition from a moderately damaged lattice to the amorphous state occurred rather abruptly. Transmission electron microscopy results confirmed the presence of the amorphous phase at fluences greater than 2×10^{15} ions·cm⁻². At 300 K, the damage (χ) reached a value of 0.66 at about 1×10^{16} ions·cm⁻² and remained there to our highest fluence of 1×10^{17} ions·cm⁻². Since Burnett and Page [5] report Al₂O₃ to be amorphous after a fluence of 2.9×10^{17} Cr·cm⁻², the curve must rise again.

To study the effect of self damage in the absence of any impurity, crystals were implanted with aluminum and oxygen ions in the ratio of 2:3 at 77 K [15]. The energies (90 keV for aluminum and 55 keV for oxygen) were chosen such that the peaks in the implanted profiles occurred at the same depth. The total ion fluence was 5×10^{16} cm⁻². An amorphous layer about 150 nm thick was produced in this case. The RBS spectra are given in Fig. 2.

That there may also be chemical effects associated with the amorphization is demonstrated by results of the zirconium implants. Figure 3 contains the RBS spectra for Al₂O₃ implanted with (a) 2×10^{16} Zr·cm⁻² and (b) 4×10^{16} Zr·cm⁻² (170 keV) at 300 K. The lattice was highly damaged but crystalline for the lower fluence. The higher fluence produced a subsurface amorphous layer extending from about 40 to 100 nm from the surface. The presence of this subsurface layer has been confirmed by TEM. As the fluence was increased to higher values, the width of the amorphous

region increased and eventually reached the specimen surface. Note that the zirconium showed no tendency to occupy substitutional lattice sites. Burnett and Page also found that the fluence of zirconium to produce the amorphous phase was a factor of ten less than the required chromium fluence [5].

To determine if the low fluence of zirconium needed to produce amorphization at this temperature was due to a mass effect or included a "chemical" component, samples were implanted with 4×10^{16} Nb·cm⁻². Figure 4 contains the RBS spectra for the niobium-implanted specimen. Neither sublattice exhibits an amorphous behavior; χ for the aluminum-sublattice is 0.7. Most (~80%) of the niobium ions were in substitutional lattice sites (as viewed along the c-axis). Because zirconium and niobium have nearly identical masses, the displacement cascades should be nearly identical. The inability of zirconium ions to occupy substitutional lattice sites may be related to its stabilization of the damage structure.

The accumulation of damage and approach to the random state (as defined by RBS) for α -SiC implanted with 62 keV nitrogen at about 300 K is shown in Fig. 5 (χ , damage in the silicon-sublattice, versus fluence). As in the case of Al₂O₃, during the early stages, the damage accumulates at a linear rate with fluence, then rises at a rate greater than linear over a relatively short fluence interval to approach the random value at about 10^{15} N·cm⁻². The fluence of chromium ions (280 keV) required to produce the random value at peak concentration depth was about 2×10^{14} ions·cm⁻², nearly an order of magnitude lower than for nitrogen. The presence of the amorphous layer has been confirmed by TEM and Raman spectroscopy for the chromium implants [16].

Implantations of nitrogen and chromium at substrate temperatures of 1023 K did not produce amorphous layers at fluences of $8 \times 10^{16} \text{ N}\cdot\text{cm}^{-2}$ and $1 \times 10^{16} \text{ Cr}\cdot\text{cm}^{-2}$, respectively.

A comparison of the fluences of chromium to produce the amorphous phases in Al_2O_3 and SiC indicates the greater susceptibility of the mostly covalent bonded SiC to amorphization. At room temperature (0.13 of the melting point of Al_2O_3 and 0.11 of the decomposition temperature of $\alpha\text{-SiC}$) a fluence of $2.9 \times 10^{17} \text{ Cr}\cdot\text{cm}^{-2}$ (300 keV) [5] or $1 \times 10^{17} \text{ Ni}\cdot\text{cm}^{-2}$ [6] was required for amorphization of Al_2O_3 compared to $2 \times 10^{14} \text{ Cr}\cdot\text{cm}^{-2}$ (280 keV) for $\alpha\text{-SiC}$.

As would be expected, the presence of an amorphous layer has a significant influence on the surface mechanical properties. The Knoop micro-indentation hardness tests were made with loads of 0.14 N (15 gf) which produced penetration depths of about 300 nm, comparable to the thickness of the amorphous layers. The measured hardness values were thus influenced by the substrate and are interpreted as indicating the minimum change in this property.

The indicated hardness of both amorphous Al_2O_3 and amorphous SiC was approximately 60% of the value for the unimplanted counterpart. Within the accuracy of these tests, the chemical nature of the implanted species had no effect. These values are consistent with our earlier work [4,16] and with those reported by Burnett and Page [5].

Scanning electron micrographs of the scratch tracks illustrate the enhanced plasticity of the amorphous phase compared to the brittle behavior of the crystalline material. Figure 6 contains the SEM photographs for scratches in Al_2O_3 made with 0.098 N (10 gf) normal loads. The debris from the crystalline sample was angular and profuse. Cracks extend for

significant distance into the substrate and often link to remove large pieces of material. On the other hand, the chips removed from the amorphous region were rounded and oftentimes curled. Cracks did not extend past the groove itself. Again there was no apparent difference between the amorphous Al_2O_3 and SiC.

CONCLUSIONS

Implantation parameters such as fluence, substrate temperature, and chemical nature of the implanted species are important in determining whether or not an amorphous phase is formed by ion implantation of Al_2O_3 and SiC. Chemical bonding in the target material is also important. In the case of Al_2O_3 , high fluences ($>10^{17}$ ions $\cdot\text{cm}^{-2}$) at room temperature or lower fluences ($\sim 10^{15}$ ions $\cdot\text{cm}^{-2}$) at 77 K produce amorphization. However only a moderate fluence of zirconium is required for room temperature amorphization. Silicon carbide at 300 K becomes amorphous at much lower fluences. The surface mechanical properties are affected by the structural changes.

ACKNOWLEDGMENT

Research sponsored by the Division of Materials Sciences, U.S. Department of Energy, under contract DE-AC05-84OR21400 with Martin Marietta Energy Systems, Inc. The authors acknowledge the aid of J. F. Pullium in conducting the scratch tests. H. Naramoto was a guest at ORNL on assignment from Japan Atomic Energy Research Institute, Tokai, Ibaraki, Japan.

REFERENCES

- 1 H. Naramoto, C. W. White, J. M. Williams, C. J. McHargue, O. W. Holland, M. M. Abraham, and B. R. Appleton, *J. Appl. Phys.* **54** (1983) 683.
- 2 H. Naramoto, C. J. McHargue, C. W. White, J. M. Williams, O. W. Holland, M. M. Abraham, and B. R. Appleton, *Nucl. Instr. Methods* **209/210** (1983) 1159.
- 3 C. W. White, G. C. Farlow, H. Naramoto, C. J. McHargue, and B. R. Appleton, *Defect Properties and Processing of High-Technology Nonmetallic Materials*, J. H. Crawford, Jr., Y. Chen, and W. A. Sibley, eds., North Holland, New York, 1984, p. 163.
- 4 C. J. McHargue, C. W. White, B. R. Appleton, G. C. Farlow, and J. M. Williams, *Ion Implantation and Ion Beam Processing of Materials*, G. K. Kubler, O. W. Holland, C. R. Clayton, and C. W. White, eds., North Holland, New York, 1984, p. 385.
- 5 P. J. Burnett and T. F. Page, *J. Mater. Sci.*, to be published.
- 6 T. Hioki, A. Itoh, S. Noda, H. Doi, J. Kawamoto, and O. Kamigaito, *Nucl. Instr. Methods B*, to be published.
- 7 H. M. Naguib and R. Kelly, *Radiat. Eff.* **25** (1975) 1.
- 8 C. Jech and R. Kelly, *J. Phys. Chem. Sol.* **30** (1969) 465; **31** (1970) 41.
- 9 H. M. Naguib, J. F. Singleton, W. A. Grant, and G. Carter, *J. Mater. Sci.* **8** (1973) 1633.
- 10 H. Matzke and J. L. Whitton, *Canad. J. Phys.* **44** (1966) 995.
- 11 M. D. Rehtin, *Radiat. Eff.* **42** (1979) 129.
- 12 O. J. Marsh, *Silicon Carbide-1973*, R. C. Marshall, J. W. Faust, Jr., and C. E. Ryan, eds., University of South Carolina Press, 1973, p. 471.
- 13 R. B. Wright, R. Varma, and D. M. Gruen, *J. Nucl. Mater.* **63** (1976) 415.
- 14 R. B. Wright and D. M. Gruen, *Radiat. Eff.* **33** (1977) 133.
- 15 C. W. White, G. C. Farlow, C. J. McHargue, P. S. Sklad, P. Angelini, and B. R. Appleton, *Nucl. Instr. Methods B*, to be published.
- 16 C. J. McHargue and J. M. Williams, *Metastable Materials Formation by Ion Implantation*, S. T. Picraux and W. J. Choyke, eds., Elsevier, 1982, p. 303.

LIST OF FIGURES

Fig. 1. Damage accumulation in the Al-sublattice during 150 keV Cr-implantation at 77 K (---) and 300 K (—). x at the depth of the peak Cr concentration is plotted as a function of fluence.

Fig. 2. Backscattering spectra of 2.0 MeV He⁺ from Al₂O₃ implanted with Al (90 keV) and O (55 keV) ions in the ratio of 3:2 at 77 K.

Fig. 3. Backscattering spectra from Al₂O₃ implanted with (a) 2×10^{16} Zr·cm⁻² and (b) 4×10^{16} Zr·cm⁻² at 300 K and 175 keV.

Fig. 4. Backscattering spectra from Al₂O₃ implanted with 4×10^{16} Nb·cm⁻² (220 keV) at 300 K.

Fig. 5. Damage accumulation in the Si-sublattice during implantation of α-SiC with 62 keV nitrogen.

Fig. 6. SEM photographs of scratches made at 0.098 N (10 gf) loads in (a) crystalline and (b) amorphous Al₂O₃.

Fig 1

NO. 340-M DIETZGEN GRAPH PAPER
MILLIMETER

FLUENCE (10¹⁵ CR IONS • CM⁻²)

EUGENE DIETZGEN CO.
MADISON, WIS. U.S.A.

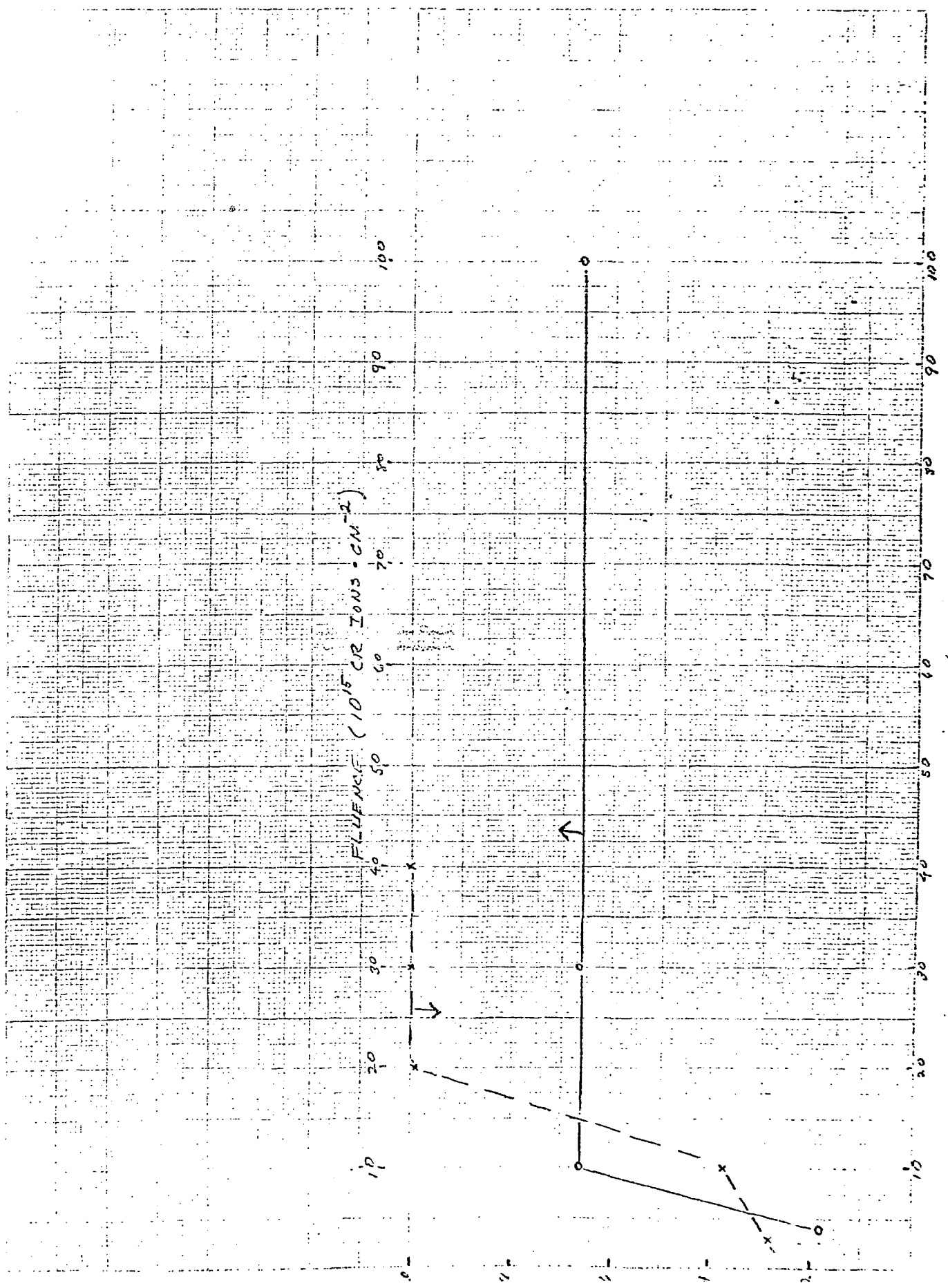
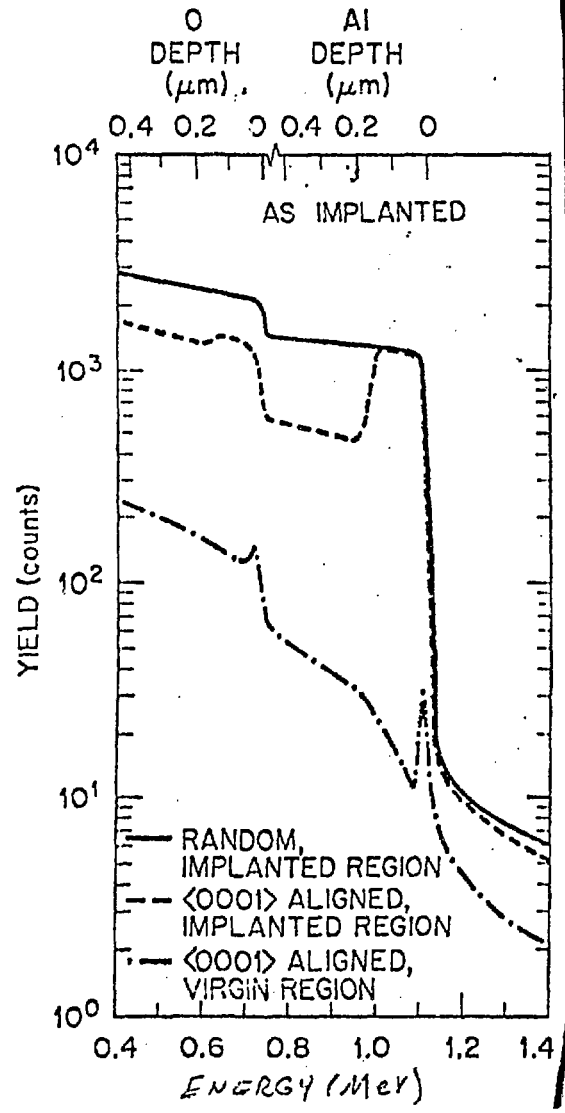
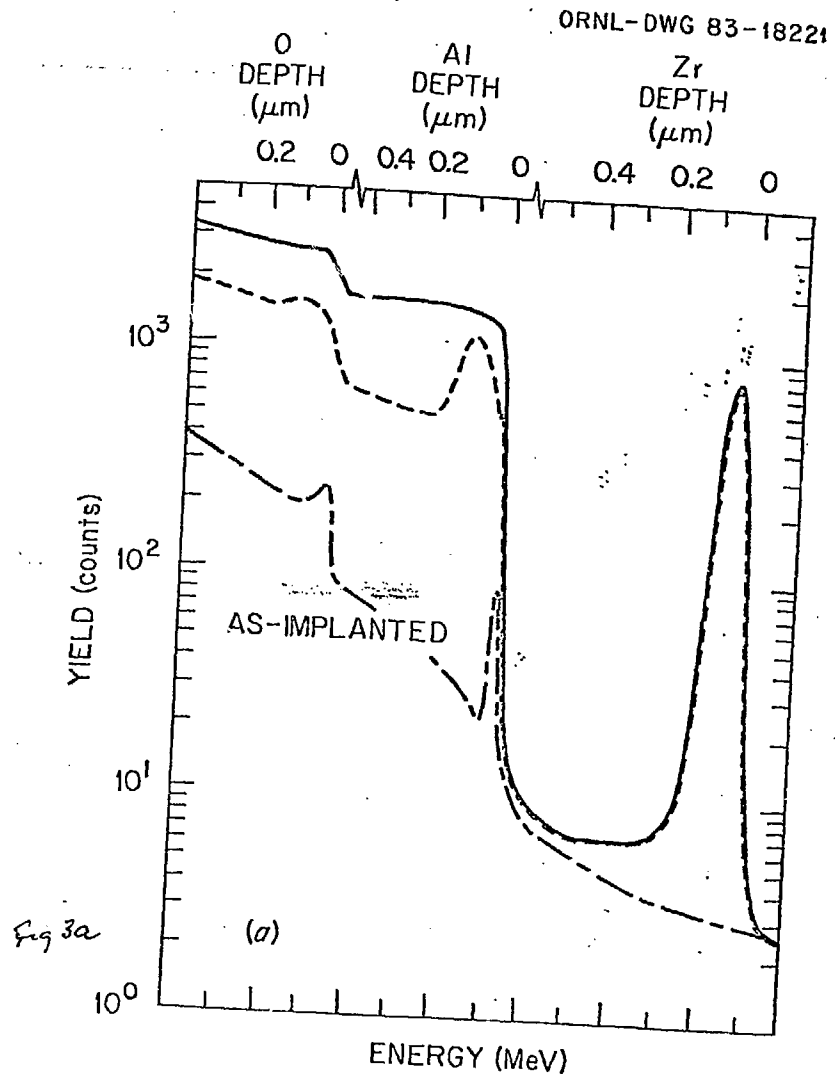
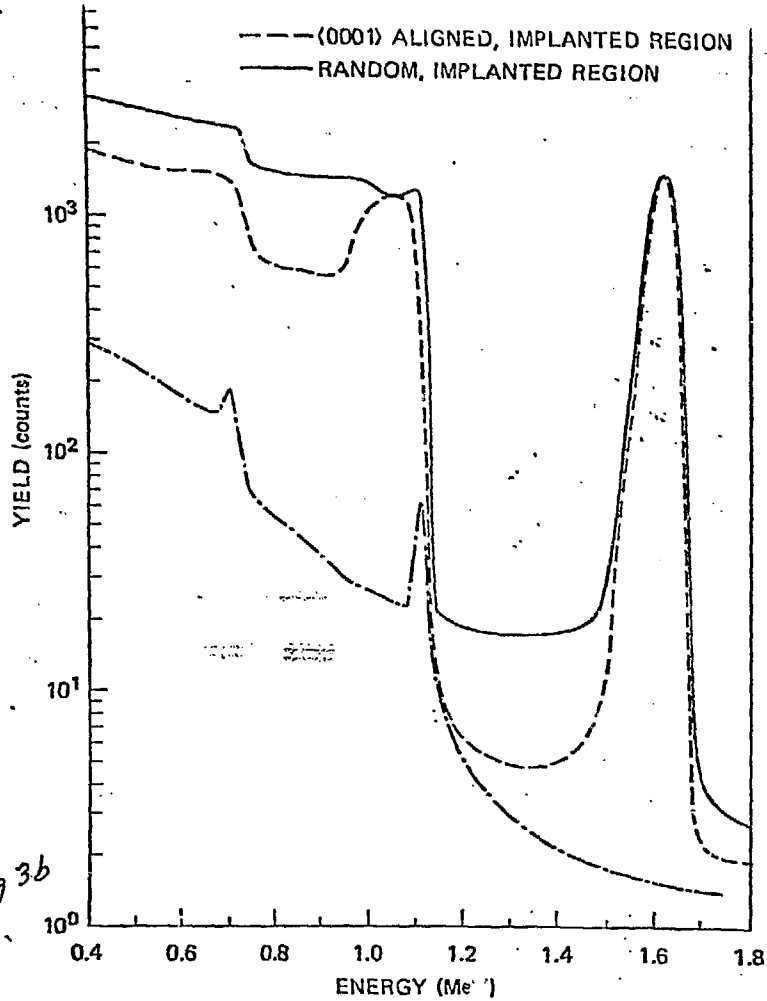
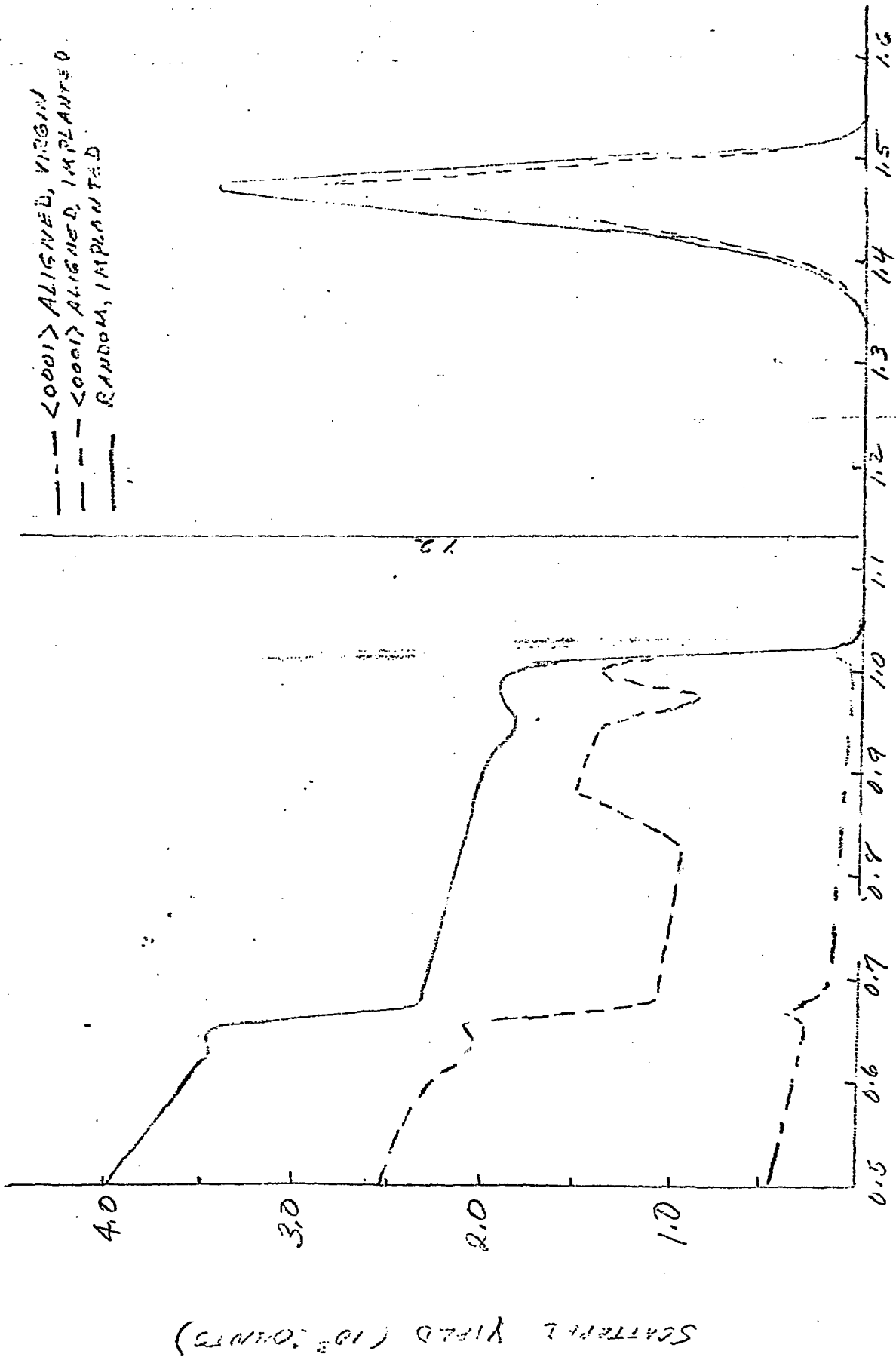




Fig. 2







ENERGY (MEV)
 Nb (220 keV, 10^{19} ions/cm²) in α -Al₂O₃

Fig 4

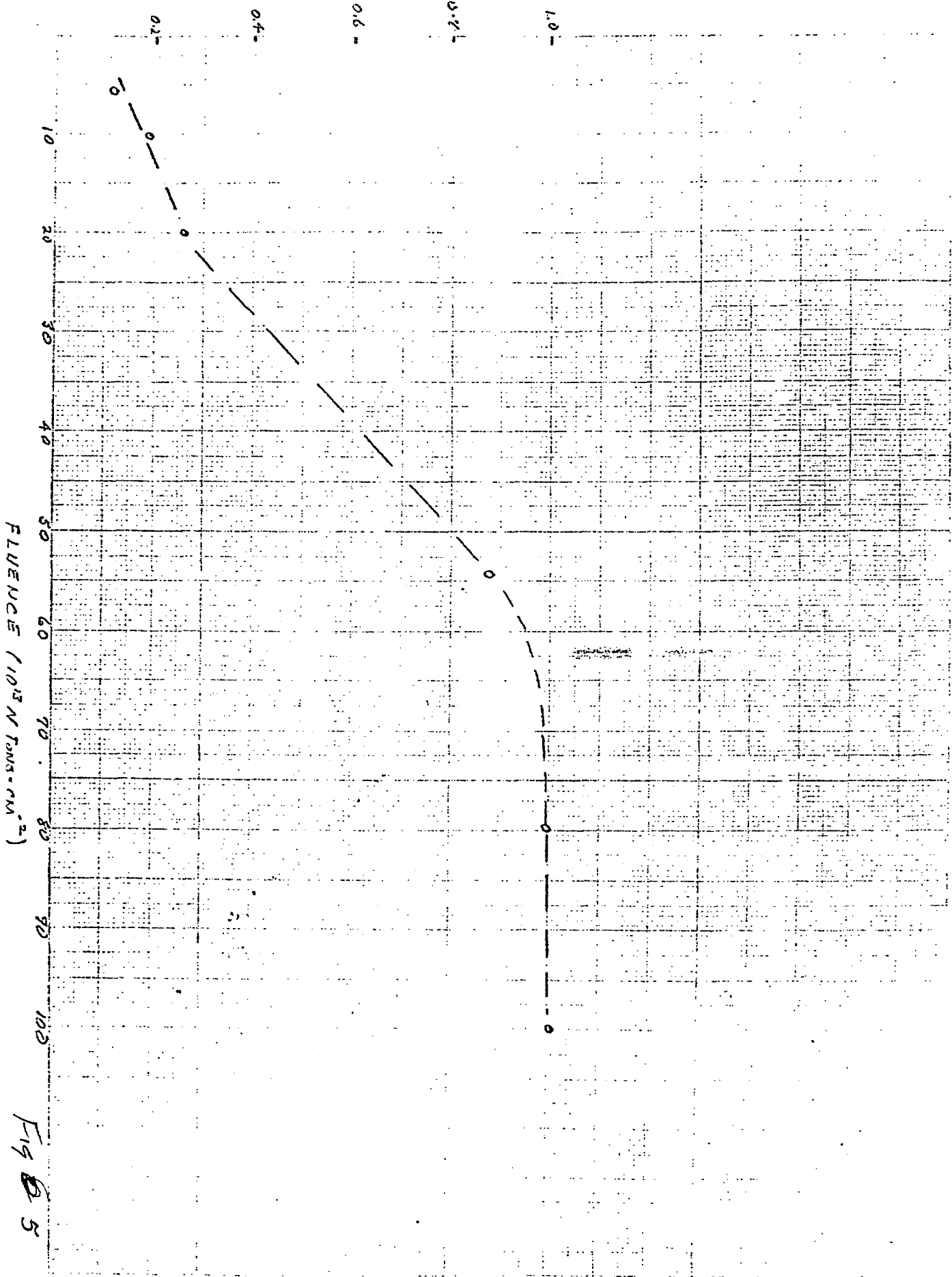
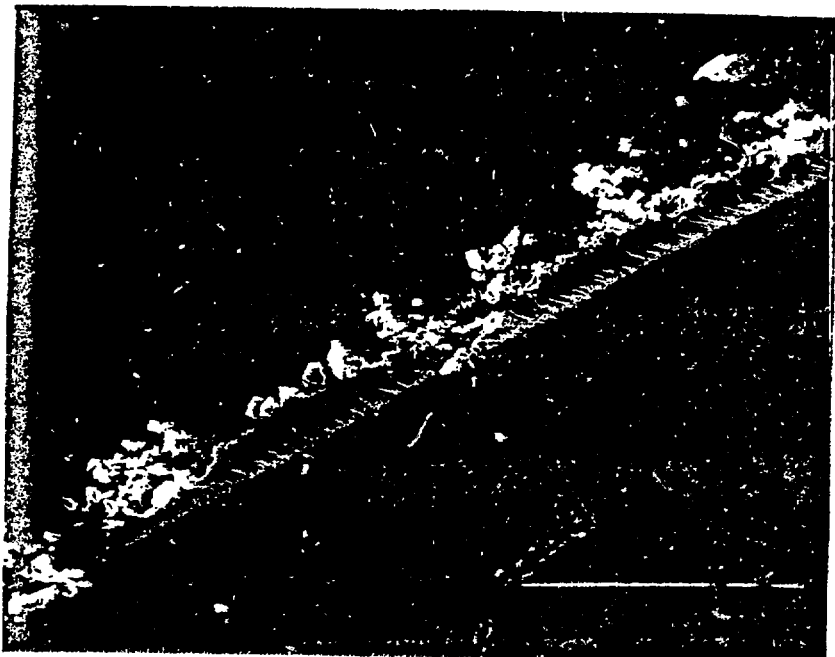
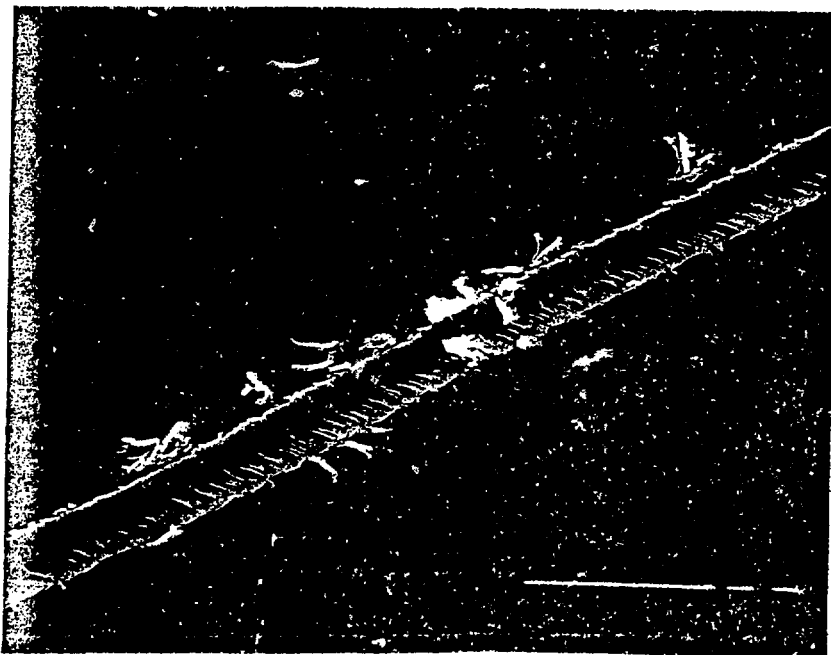


Fig 5



(a)



(b)

7296